# Absolute partial and total electron impact ionization cross sections for $CF_4$ from threshold up to 180 eV

K. Stephan,[a] H. Deutsch,[b] and T. D. Märk
*Institut für Experimentalphysik, Leopold Franzens Universität, A 6020 Innsbruck, Austria*

(Received 2 May 1985; accepted 7 August 1985)

Electron impact ionization of carbon tetrafluoride was studied as a function of electron energy from threshold up to 180 eV. A double focusing mass spectrometer system with an improved electron impact ion source was used, alleviating the problems of ion extraction from the source and the transmission of the extracted ions through the mass spectrometer system. Absolute partial ionization cross section functions for the production of $CF_3^+$, $CF_2^+$, $CF^+$, $C^+$, $F^+$, $CF_3^{2+}$, and $CF_2^{2+}$ in $CF_4$ have been determined. In addition, the total (and the counting) ionization cross section function of $CF_4$ has been determined (summation method) and is compared with calculations based on classical and semiclassical binary encounter approximations. Using *n*th root extrapolation ionization energies of the following doubly charged fragment ions have been derived: AE $(CF_3^{2+}) = 41.8 \pm 0.3$ eV, AE $(CF_2^{2+}) = 42.9 \pm 0.3$ eV, and AE $(CF^{2+}) = 52.1 \pm 0.5$ eV. In accordance with previous results no stable $CF_4^+$ parent ion has been detected, however, a metastable dissociation process $CF_4^{+*} \rightarrow CF_3^+ + F$ has been observed.

## I. INTRODUCTION

The present study—one in a series from this laboratory supplying quantitative knowledge on electron impact ionization[1]—is devoted to carbontetrafluoride. Recently, there has been growing interest in the properties of halocarbon compounds used for plasma etching[2] and several studies have been reported on glow discharges operating with $CF_4$.[3] Therefore we have extended our previous study on $CCl_4$[4] in the present investigation to $CF_4$ using an improved ion beam-deflection technique to measure quantitatively the fragment ions of $CF_4$ in a double focusing mass spectrometer.

A number of electron impact, photoionization, and photoelectron spectroscopy studies[5–7] have been made on $CF_4$ reporting the observation of various positive and negative ions and some of their properties. Single ionization by electron impact of $CF_4$ near threshold, yielding appearance energies, has been studied by several authors,[8] but to the authors' knowledge only one experimental determination[9] of appearance energies for the doubly charged fragment ions $CF_3^{2+}$ and $CF_2^{2+}$ in $CF_4$ is available yet. There exists one electron impact ionization study[10] which gives relative ion current abundances of the positive and negative fragment ions of $CF_4$ (i.e., $CF_3^+$, $CF_2^+$, $CF^+$, $C^+$, $F^+$,$CF_3^-$, $F^-$). A parent molecular ion $CF_4^+$ has not been observed in $CF_4$[5] and the observation of large, single valued kinetic energy releases for $CF_3^+$ with no increase as the internal energy increases has lead to the suggestion that in the production of $CF_3^+$ "some sort of predissociation is involved",[5] and not only prompt dissociation of $CF_4^+$ $(X\,^2T_1)$ and $CF_4^+$ $(A\,^2T_2)$ is responsible for this lack of parent $CF_4^+$ in the mass spectra observed. Beran and Kevan[11] have measured total ionization cross sections of $CF_4$ at an electron energy of 70, 35, and 20 eV, respectively. Other important information about electron impact interaction with $CF_4$ or fragment radicals of $CF_4$ comes from recent studies on total electron impact dissociation cross sections of $CF_4$[12] and on partial electron impact ionization cross sections of $CF_3$ radicals.[13]

In the present paper absolute partial electron impact ionization cross sections have been determined from threshold up to 180 eV for the following fragment ions of $CF_4$:$CF_3^+$, $CF_2^+$, $CF^+$, $C^+$, $F^+$, $CF_3^{2+}$, and $CF_2^{2+}$. For these measurements the previously developed technique for measuring accurate partial ionization cross sections and ratios of *parent* ions[14] has been further improved and adapted to allow quantitative detection of *fragment* ions with excess kinetic energy. In addition, the appearance energies for the doubly charged fragment ions $CF_3^{2+}$, $CF_2^{2+}$, and $CF^{2+}$ have been measured using the method of *n*th root extrapolation.

## II. EXPERIMENTAL

### A. Apparatus

The experimental system used consists of a conventional three-electrode-type electron impact ion source (Nier type), a high-resolution double focusing (reversed geometry sector field) mass spectrometer, and a gas handling system. The properties of the ion source and mass spectrometer have been studied in detail previously and essential improvements in the performance could be achieved.[14] With help of these improved operating conditions it was possible to measure with high accuracy absolute partial ionization cross sections for *parent* ions.[14] In the present study the method was extended to allow the measurement of partial ionization cross sections for *fragment* ions with excess kinetic energy.

Figure 1 gives a schematic view of the electron impact ion source and the ion extraction and focusing system used. The gas under study ($CF_4$ or Ar) flows from a reservoir through a 10 $\mu$m diameter nozzle $N$ into the high vacuum region (background pressure $\sim 10^{-7}$ Torr). Approximately

[a] Permanent address: Universitätsklinik für Hör-, Stimm-, und Sprachstörungen, Leopold Franzens Universität, A 6020 Innsbruck, Austria.
[b] Permanent address: Sektion Physik/Elektronik, Ernst Moritz Arndt Universität, DDR-22 Greifswald, West Germany.

 0021-9606/85/235712-09$02.10 

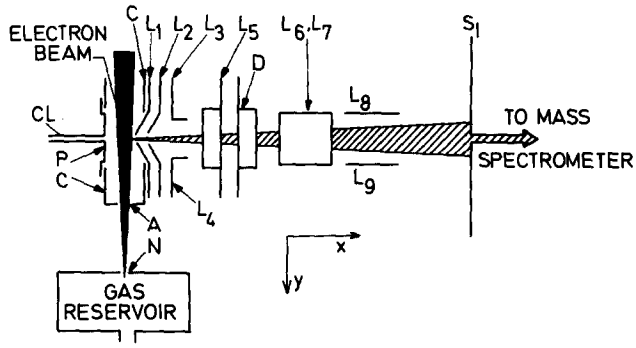


FIG. 1. Schematic drawing of the electron impact ion source used in the present study. P: pusher, C: collision chamber, CL: capillary leak gas inlet, A: aperture, N: nozzle for molecular beam gas inlet, $L_1$: collision chamber exit slit electrodes, $L_2$: penetrating field electrodes (see the text), $L_3$ and $L_4$: focusing electrodes, $L_5$: grounded slit, D: defining aperture, $L_6$, $L_7$, $L_8$, and $L_9$: deflection electrodes (see the text), $S_1$: mass spectrometer entrance slit. $z$ direction perpendicular to the $x$–$y$ plane (right-hand axes).

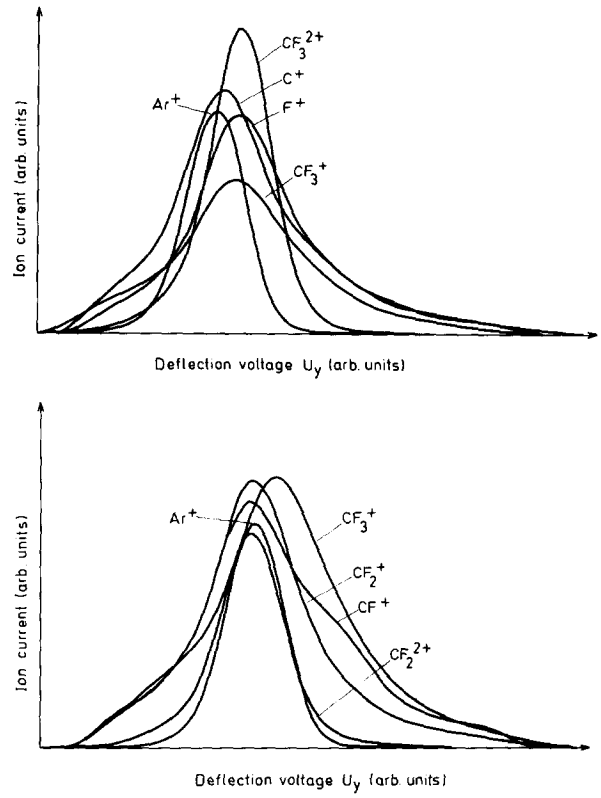


FIG. 2. Ion beam profiles (deflection curves in $y$ direction) of $Ar^+$ and fragment ions of $CF_4$ obtained by sweeping the fanned out ion beam perpendicular across the mass spectrometer entrance slit $S_1$ with help of deflection plates $L_8$ and $L_9$ (see Fig. 1) under strong focusing conditions of $L_3$ and $L_4$ (see the text). Electron energy: 100 eV. Curves are not normalized and are displaced arbitrarily in $U_y$ direction. It can be seen that the width of the fragment ion beam profiles is increasing with decreasing ion mass, since the kinetic excess energy of dissociative ions with smaller mass is larger. For comparison see kinetic energy distribution of $CF_3^+$ and $CF_2^+$ produced by electron impact ionization of $CF_4$ reported previously by Dibeler *et al.* (Ref. 10). Moreover, doubly charged fragment ions have a smaller ion beam profile than singly charged fragment ions.

20 mm downstream a fraction of the emerging molecular beam enters the collision chamber C through a 5 mm diameter aperture A and is crossed at right angles by an electron beam of variable energy (up to 180 eV). A 500 $\ell$/s turbomolecular pump evacuates the open ion chamber. The electron beam (with stabilized currents between 1 and 30 $\mu$A) is aligned by a weak magnetic field ($\sim$400 G). The energy spread of the electron beam is approximately 0.5 eV (FWHM).[14]

Ions formed by electron impact are extracted from the collision chamber through a slit in electrode $L_1$ [1.5 mm width in $y$ direction (see Fig. 1), 8 mm height in $z$ direction] with help of an electric field penetrating into the collision chamber from $L_2$. $L_1$, pusher P and the collision chamber C are kept at the potential of C, typically + 3 kV (ion accelerating voltage). $L_3$ and $L_4$ are used for beam centering and focusing, $L_5$ is the end of the accelerating region, and D is a defining aperture. Deflection plates $L_6$, $L_7$ and $L_8$, $L_9$ serve to sweep the extracted ion beam either parallel ($z$ deflection) or perpendicular ($y$ deflection) across the mass spectrometer entrance slit $S_1$, respectively. The fraction of ions passing $S_1$ is analyzed in a 90° magnetic sector field followed by a 90° electric sector field. In addition to a Faraday cup, which is used to measure absolute ion currents (in order to determine all absolute cross sections and ratios; see Sec. II C), a CuBe-conversion dynode followed by a channeltron is used as either analog or counting ion detector.

### B. Experimental method

In order to determine *absolute* partial ionization cross sections it is necessary to uniquely correlate the mass analyzed ion signal at the ion collecting system (either Faraday cup or channeltron) to the number of ions produced in the ion source at a known target gas density and for a known electron beam current. As has been noted previously[14] this is a difficult task due to mass to charge dependent discrimination in the extraction of the ions from the ion source and at the entrance slit $S_1$ of the mass spectrometer.

In order to avoid the latter it has been shown[14] that for ions originating without kinetic energy (parent ions) it is sufficient to sweep the extracted ion current with help of $L_{8,9}$ perpendicular to $S_1$ and to integrate over the recorded $y$-ion beam profile. Figure 2 shows $y$-ion beam profiles for $Ar^+$ and $CF_4$ fragment ions. It can clearly be seen that different ions have different beam shapes and centers leading to discrimination without integration.[14]

Because of negligible differences in $z$-ion beam profiles for *parent* ions no integration parallel to $S_1$ was necessary previously.[14] For *fragment* ions, however, e.g., $CF_4$ fragment ions, also discrimination in the $z$ direction has to be accounted for because of large differences in the $z$-ion beam profiles for different species. Figure 3 shows $z$-ion beam profiles for singly and doubly charged ions of $CF_4$. Without integration large discrimination effects will occur in the detection efficiency of ions with different mass to charge ratio and different excess kinetic energy.

Figures 4 and 5 show the two dimensional $Ar^+$ and $CF_3^+$ ion beam shape, respectively, obtained by various scans in $y$ and $z$ direction. It can be seen that the ion beam shape is essentially a product of the profiles in either direction. Thus, in order to account for the overall discrimination

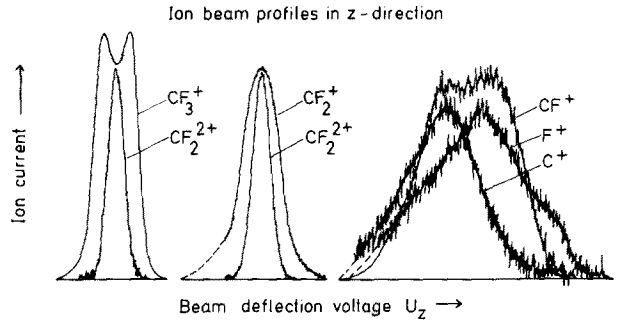


FIG. 3. Ion beam profiles (deflection curves in $z$ direction) of fragment ions of $CF_4$ obtained by sweeping the fanned out ion beam across the mass spectrometer entrance slit $S_1$ with help of the deflection plates $L_{6,7}$ under strong focusing conditions of $L_3$ and $L_4$ (see the text). Electron energy: 100 eV. It can be seen that the width of the fragment ion beam profiles is increasing with decreasing ion mass, since the kinetic excess energy of dissociative ions with smaller mass is larger. Moreover, doubly charged fragment ions have a smaller ion beam profile than singly charged fragment ions. (See also difference between $Ar^+$ and $Ar^{2+}$ profile in Ref. 14.)

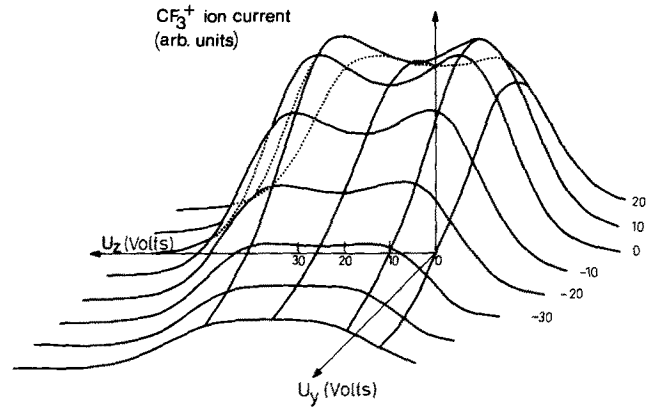


FIG. 5. $CF_3^+$ current as a function of the deflection voltage $U_y$ and $U_z$. Electron energy: 70 eV.

it is sufficient to determine the profile in $z$ direction at one particular $y$ value (e.g., $U_y = OV$) and the profile in $y$ direction at one particular $z$ value (e.g., $U_z = OV$) and then integrate over the whole beam shape.

Moreover, it is not only necessary to avoid any discrimination at $S_1$, but it is also necessary to extract all ions of a specific species produced in the ion source in order to obtain reliable ion current ratios and/or cross section ratios. Stephan *et al.*[14] have demonstrated that this is possible for parent ions, if the field penetration from lens $L_2$ into the collision chamber is strong enough and integration over the $y$-ion beam profile is performed. In the present investigation we have studied the extraction conditions for fragment ions and Fig. 6 gives the experimental proof that mass analyzed $y$-integrated ion signals not only saturate for parent ions (e.g., $Ar^+$ given in Fig. 6), but also for fragment ions (e.g., $CF_3^+$ given in Fig. 6) if the potential differences between the collision chamber and lens $L_2$, $U_{C\text{-}L_2}$, is large enough. Ion current and/or cross section ratio measurements have been made under saturation–extraction conditions and using the above described integration over $y$ and $z$ direction.

As shown previously,[14] ion beam profiles also depend on the potentials of the extraction lens $L_2$ and the focusing lenses $L_3$ and $L_4$. Ion beam profiles given in Figs. 2 through 5 have been measured under "strong" extraction conditions (which were necessary for the measurement of cross section ratios, i.e., saturation conditions). However, if the voltages between collision chamber and $L_2$, $L_3$, and $L_4$ are lowered, broad ion beam profiles are obtained (e.g., see Fig. 7), which do not significantly change their shape as the electron energy is varied. This condition, for which the ion extraction and discrimination effects are independent of the electron energy, is used for measuring the relative cross section functions.[14] Ion current and the gas pressure in the ion source and in the gas reservior (which were kept constant) were recorded simultaneously in a data acquisition unit. Typically in one run a total of 400 values of each of these parameters were recorded at about 100 different values of electron energy.

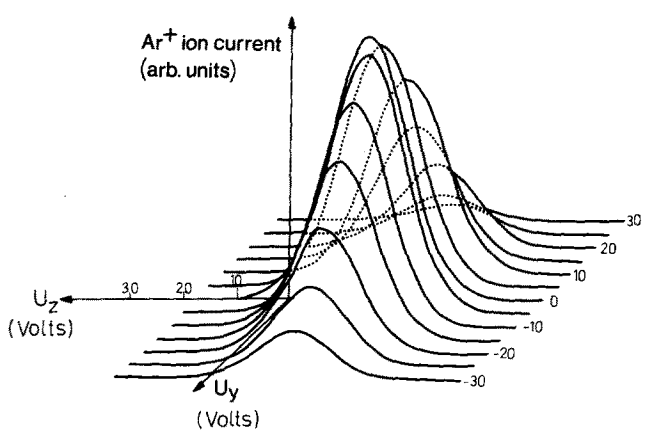


FIG. 4. $Ar^+$ current as a function of the deflection voltage $U_y$ and $U_z$ (with $U_y = U_{L_5} - U_{L_4}$ and $U_z = U_{L_6} - U_{L_7}$). Electron energy: 70 eV.

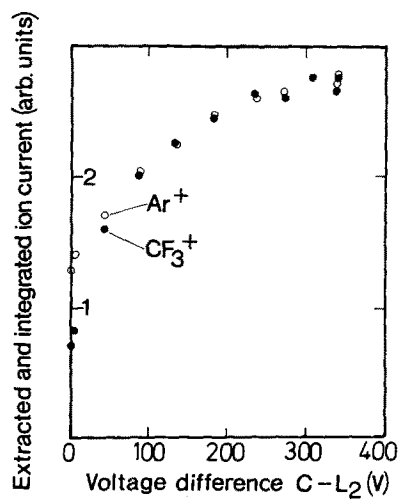


FIG. 6. $y$-integrated ion current as a function of the potential difference between the collision chamber C and the lens $L_2$, $U_{C\text{-}L_2}$.

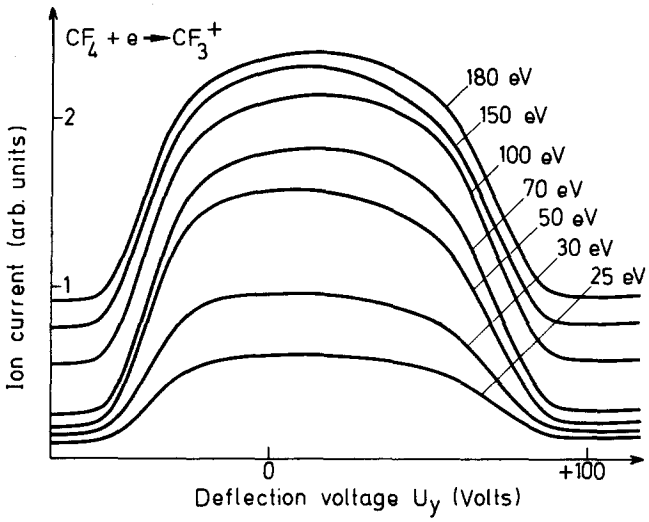


FIG. 7. Ion beam profiles (deflection curves in $y$ direction) of $CF_3^+$ obtained under weak extraction conditions (see the text) at different electron energies.

### C. Calibrations

The energy scales of the singly charged $CF_4$ fragment ions are absolutely calibrated using linear extrapolation of the $Ar^+$ cross section to the ionization energy of $Ar^+$ (15, 76 eV[8]), whereas the energy scales of the doubly charged fragment ions of $CF_4$ are calibrated against the $Ar^{2+}$ cross section onset of 43.4 eV [8] using the square root extrapolation method.

The absolute calibration of the measured relative partial ionization cross section functions is a difficult experimental task,[1,15] because it necessitates the accurate measurement of the ion current, the number gas density, the collision path length, and the current of the bombarding electrons. Instead we have used a normalization procedure in which the cross section to be determined, e.g., $q(CF_3^+/CF_4)$, is normalized against the $Ar^+$ cross section[14] at one particular electron energy, i.e., the electron impact ionization is measured for both gases (ions) under identical conditions (collision path length and electron current) and for known gas densities, and hence the measured ion current ratio corrected for the respective gas densities can be set equal to the corresponding cross section ratio.

This normalization requires the measurement of the gas density of Ar and $CF_4$ in the collision chamber, which was made with help of the method of molecular effusive flow.[16,18] This method relies on the validity of free (collisionless) molecular effusive flow (Knudsen number $K = \lambda_0/D > 10$, with $\lambda_0$ mean free path of the gas and $D$ diameter of orifice) from the gas reservoir through the nozzle into the collision chamber and from there to the high vacuum pumps. Under these conditions the gas density ratio in the collision chamber $Ar/CF_4$ is equal to the pressure ratio in the gas reservoir $p(Ar)/p(CF_4)$. Moreover, in order to eliminate any pressure effects the $y$ ion beam profiles of the respective ion signals were measured and integrated for a series of different gas reservoir pressures. The resulting averaged ion current ratios were corrected with help of measured and integrated $z$ profiles. This gives a cross section ratio (at 70 eV) of $q(CF_3^+/CF_4)/q(Ar^+/Ar) = 1.12$, i.e., yielding with help of $q(Ar^+/Ar) = 2.54\times10^{-20}$ m$^2$ [14] a value of $q(CF_3^+/CF_4) = 2.84\times10^{-20}$ m$^2$. This calibration procedure involves an estimated error of $\pm$ 5 to 10%. Similarly, the other fragment ions of $CF_4$ have been calibrated (at one pressure) against $CF_3^+$ yielding the cross section ratios at 100 eV electron energy given in Table I.

TABLE I. Measured cross section ratios in percent for $CF_4$ fragment ions at 100 eV electron energy (see the text for method).

| | |
|---|---|
| $q(CF_2^+/CF_4)/q(CF_3^+/CF_4)$ | 7.21 |
| $q(CF^+/CF_4)/q(CF_3^+/CF_4)$ | 4.07 |
| $q(C^+/CF_4)/q(CF_3^+/CF_4)$ | 2.54 |
| $q(F^+/CF_4)/q(CF_3^+/CF_4)$ | 2.98 |
| $q(CF_3^{2+}/CF_4)/q(CF_3^+/CF_4)$ | 0.31 |
| $q(CF_2^{2+}/CF_4)/q(CF_3^+/CF_4)$ | 0.76 |

## III. RESULTS AND DISCUSSION

In the electron impact mass spectrum of $CF_4$ (at 100 eV electron energy) there are only fragment ions, the dominant of which is $CF_3^+$. There is no evidence for the presence of stable ($\geq$10 $\mu$s) $CF_4^+$ in our experiment. This is in accordance with earlier electron and photon ionization studies of $CF_4$.[5] We have, however, investigated a possible inflight de-

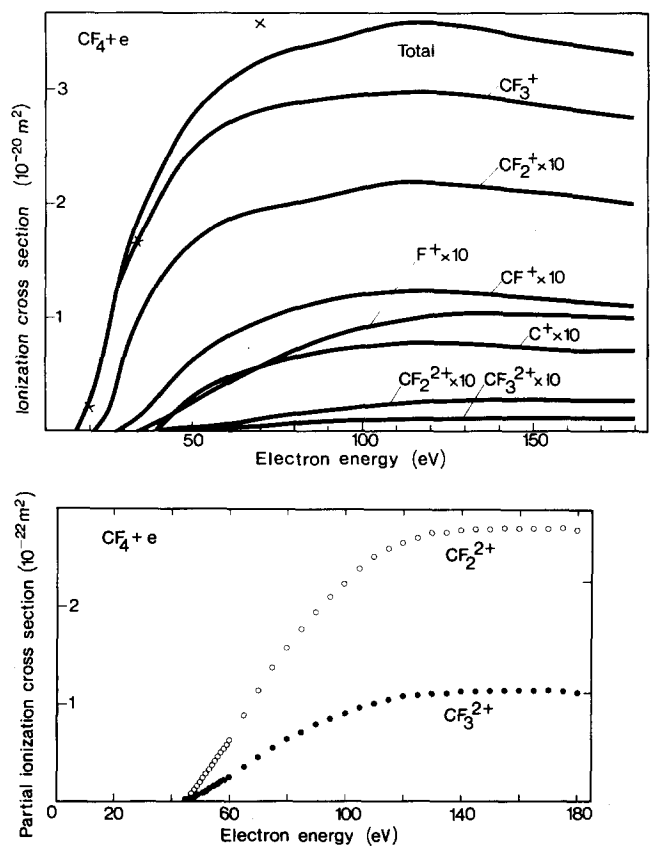


FIG. 8. Absolute partial and total ionization cross sections in $CF_4$ as a function of electron energy. Crosses: total ionization cross section values reported by Beran and Kevan (Ref. 11) recalibrated with help of data reported by Rapp and Englander-Golden (Ref. 17) (see the text).

TABLE II. Absolute partial, total, and counting ionization cross sections in $10^{-20}$ m$^2$ for $CF_4$ as a function of electron energy in eV.

| Electron energy | $q$ (counting) | $q$ (total) | $q(CF_3^+/CF_4)$ | $q(CF_2^+/CF_4)$ | $q(CF^+/CF_4)$ | $q(C^+/CF_4)$ | $q(F^+/CF_4)$ | $q(CF_3^{2+}/CF_4)$ | $q(CF_2^{2+}/CF_4)$ |
|---|---|---|---|---|---|---|---|---|---|
| 16 | 0.0114 | 0.0114 | 0.0114 | | | | | | |
| 17 | 0.0390 | 0.0390 | 0.0390 | | | | | | |
| 18 | 0.087 | 0.087 | 0.087 | | | | | | |
| 19 | 0.153 | 0.153 | 0.153 | | | | | | |
| 20 | 0.231 | 0.231 | 0.231 | | | | | | |
| 21 | 0.321 | 0.321 | 0.321 | 0.000 354 | | | | | |
| 22 | 0.425 | 0.425 | 0.423 | 0.001 39 | | | | | |
| 23 | 0.54 | 0.54 | 0.530 | 0.004 59 | | | | | |
| 24 | 0.66 | 0.66 | 0.65 | 0.009 1 | | | | | |
| 25 | 0.79 | 0.79 | 0.78 | 0.015 2 | | | | | |
| 26 | 0.93 | 0.93 | 0.91 | 0.022 8 | 0.000 099 | | | | |
| 27 | 1.07 | 1.07 | 1.04 | 0.031 5 | 0.000 186 | | | | |
| 28 | 1.21 | 1.21 | 1.17 | 0.041 8 | 0.000 237 | | | | |
| 29 | 1.35 | 1.35 | 1.30 | 0.056 | 0.000 332 | | | | |
| 30 | 1.48 | 1.48 | 1.41 | 0.070 | 0.000 55 | | | | |
| 31 | 1.60 | 1.60 | 1.52 | 0.086 | 0.001 15 | | | | |
| 32 | 1.69 | 1.69 | 1.59 | 0.100 | 0.002 21 | | | | |
| 33 | 1.78 | 1.78 | 1.66 | 0.111 | 0.003 75 | | | | |
| 34 | 1.86 | 1.86 | 1.73 | 0.120 | 0.006 1 | 0.000 0127 | 0.000 204 | | |
| 35 | 1.93 | 1.93 | 1.80 | 0.125 | 0.009 1 | 0.000 146 | 0.000 264 | | |
| 36 | 2.00 | 2.00 | 1.86 | 0.128 | 0.012 4 | 0.000 54 | 0.000 445 | | |
| 37 | 2.06 | 2.06 | 1.91 | 0.129 | 0.015 9 | 0.001 12 | 0.000 76 | | |
| 38 | 2.11 | 2.11 | 1.96 | 0.129 | 0.019 7 | 0.001 84 | 0.001 12 | | |
| 39 | 2.17 | 2.17 | 2.01 | 0.129 | 0.023 6 | 0.003 59 | 0.001 89 | | |
| 40 | 2.23 | 2.23 | 2.06 | 0.130 | 0.027 6 | 0.005 5 | 0.002 97 | | |
| 41 | 2.29 | 2.29 | 2.11 | 0.132 | 0.032 0 | 0.007 7 | 0.004 34 | 0.000 0156 | |
| 42 | 2.35 | 2.35 | 2.16 | 0.135 | 0.036 4 | 0.010 2 | 0.005 9 | 0.000 0343 | 0.000 003 09 |
| 43 | 2.42 | 2.42 | 2.21 | 0.139 | 0.040 9 | 0.133 | 0.007 8 | 0.000 063 | 0.000 035 7 |
| 44 | 2.48 | 2.48 | 2.27 | 0.144 | 0.046 3 | 0.016 6 | 0.010 0 | 0.000 116 | 0.000 131 |
| 45 | 2.54 | 2.55 | 2.31 | 0.148 | 0.051 0 | 0.019 7 | 0.012 7 | 0.000 185 | 0.000 267 |
| 46 | 2.60 | 2.60 | 2.36 | 0.152 | 0.055 | 0.022 8 | 0.015 5 | 0.000 270 | 0.000 53 |
| 47 | 2.66 | 2.66 | 2.40 | 0.156 | 0.059 | 0.026 0 | 0.018 2 | 0.000 386 | 0.00 83 |
| 48 | 2.71 | 2.71 | 2.43 | 0.160 | 0.062 | 0.028 8 | 0.020 6 | 0.000 52 | 0.001 17 |
| 49 | 2.75 | 2.75 | 2.47 | 0.163 | 0.065 | 0.031 4 | 0.022 7 | 0.000 67 | 0.001 53 |
| 50 | 2.79 | 2.80 | 2.50 | 0.167 | 0.067 | 0.033 7 | 0.025 0 | 0.000 82 | 0.001 93 |
| 51 | 2.83 | 2.84 | 2.53 | 0.170 | 0.069 | 0.035 5 | 0.026 8 | 0.000 96 | 0.002 37 |
| 52 | 2.87 | 2.87 | 2.56 | 0.172 | 0.071 | 0.037 2 | 0.028 5 | 0.001 08 | 0.002 77 |
| 53 | 2.90 | 2.91 | 2.58 | 0.175 | 0.072 | 0.038 6 | 0.030 3 | 0.001 26 | 0.003 20 |
| 54 | 2.94 | 2.94 | 2.61 | 0.177 | 0.074 | 0.039 7 | 0.031 7 | 0.001 41 | 0.003 63 |
| 55 | 2.96 | 2.97 | 2.63 | 0.179 | 0.076 | 0.040 7 | 0.033 1 | 0.001 55 | 0.004 07 |
| 56 | 2.99 | 3.00 | 2.65 | 0.180 | 0.077 | 0.041 8 | 0.034 5 | 0.001 76 | 0.004 50 |
| 57 | 3.02 | 3.02 | 2.67 | 0.182 | 0.078 | 0.043 0 | 0.035 9 | 0.001 95 | 0.004 90 |
| 58 | 3.04 | 3.05 | 2.69 | 0.184 | 0.080 | 0.044 2 | 0.037 4 | 0.002 11 | 0.005 3 |
| 59 | 3.06 | 3.07 | 2.70 | 0.186 | 0.082 | 0.045 4 | 0.038 9 | 0.002 26 | 0.005 7 |
| 60 | 3.09 | 3.10 | 2.72 | 0.187 | 0.083 | 0.046 7 | 0.040 5 | 0.002 47 | 0.006 2 |
| 65 | 3.19 | 3.20 | 2.79 | 0.193 | 0.091 | 0.053 | 0.049 0 | 0.003 51 | 0.008 7 |
| 70 | 3.26 | 3.28 | 2.84 | 0.199 | 0.098 | 0.058 | 0.056 | 0.004 53 | 0.019 3 |

TABLE II (*continued*)

| Electron energy | $q$ (counting) | $q$ (total) | $q(CF_3^+/CF_4)$ | $q(CF_2^+/CF_4)$ | $q(CF^+/CF_4)$ | $q(C^+/CF_4)$ | $q(F^+/CF_4)$ | $q(CF_3^{2+}/CF_4)$ | $q(CF_2^{2+}/CF_4)$ |
|---|---|---|---|---|---|---|---|---|---|
| 75 | 3.31 | 3.33 | 2.86 | 0.201 | 0.104 | 0.062 | 0.063 | 0.005 4 | 0.013 6 |
| 80 | 3.36 | 3.38 | 2.89 | 0.204 | 0.109 | 0.065 | 0.070 | 0.006 3 | 0.015 7 |
| 85 | 3.40 | 3.42 | 2.91 | 0.207 | 0.112 | 0.068 | 0.075 | 0.007 0 | 0.017 6 |
| 90 | 3.44 | 3.46 | 2.93 | 0.210 | 0.116 | 0.070 | 0.080 | 0.007 8 | 0.019 3 |
| 95 | 3.47 | 3.50 | 2.95 | 0.211 | 0.119 | 0.073 | 0.085 | 0.008 4 | 0.020 7 |
| 100 | 3.49 | 3.52 | 2.96 | 0.213 | 0.121 | 0.074 | 0.089 | 0.008 9 | 0.022 2 |
| 105 | 3.54 | 3.58 | 3.00 | 0.218 | 0.123 | 0.076 | 0.093 | 0.009 5 | 0.023 7 |
| 110 | 3.56 | 3.60 | 3.01 | 0.220 | 0.124 | 0.077 | 0.097 | 0.010 0 | 0.024 9 |
| 115 | 3.58 | 3.62 | 3.02 | 0.219 | 0.125 | 0.077 | 0.099 | 0.010 3 | 0.025 7 |
| 120 | 3.56 | 3.60 | 3.01 | 0.218 | 0.125 | 0.078 | 0.100 | 0.010 7 | 0.026 3 |
| 125 | 3.55 | 3.59 | 2.99 | 0.127 | 0.124 | 0.078 | 0.101 | 0.010 9 | 0.026 8 |
| 130 | 3.52 | 3.56 | 2.97 | 0.216 | 0.122 | 0.077 | 0.101 | 0.010 9 | 0.027 3 |
| 135 | 3.50 | 3.54 | 2.95 | 0.214 | 0.121 | 0.076 | 0.101 | 0.011 0 | 0.027 4 |
| 140 | 3.48 | 3.52 | 2.93 | 0.213 | 0.119 | 0.075 | 0.101 | 0.011 2 | 0.027 6 |
| 145 | 3.46 | 3.50 | 2.92 | 0.211 | 0.118 | 0.075 | 0.101 | 0.011 2 | 0.022 7 |
| 150 | 3.44 | 3.48 | 2.90 | 0.211 | 0.117 | 0.074 | 0.101 | 0.011 2 | 0.027 7 |
| 155 | 3.41 | 3.45 | 2.87 | 0.209 | 0.115 | 0.073 | 0.101 | 0.011 3 | 0.027 8 |
| 160 | 3.39 | 3.43 | 2.85 | 0.209 | 0.114 | 0.073 | 0.101 | 0.011 3 | 0.027 8 |
| 165 | 3.36 | 3.40 | 2.83 | 0.207 | 0.113 | 0.072 | 0.100 | 0.011 3 | 0.027 8 |
| 170 | 3.34 | 3.38 | 2.81 | 0.205 | 0.112 | 0.072 | 0.100 | 0.011 3 | 0.017 8 |
| 175 | 3.32 | 3.36 | 2.79 | 0.203 | 0.112 | 0.072 | 0.100 | 0.011 2 | 0.027 8 |
| 180 | 3.30 | 3.33 | 2.78 | 0.200 | 0.110 | 0.071 | 0.099 | 0.011 1 | 0.027 8 |

TABLE III. Fragment ion current intensities in $CF_4$ at 70 eV electron energy as percentage of the $CF_3^+$ ion.

| Ion | Dibeler *et al.* (Ref. 10) | Present |
|---|---|---|
| $CF_3^+$ | 100 | 100 |
| $CF_2^+$ | 14.5 | 6.9 |
| $CF^+$ | 3.7 | 3.5 |
| $C^+$ | 9.4 | 2.0 |
| $F^+$ | 5.7 | 1.97 |
| $CF_3^{2+}$ | ... | 0.3 |
| $CF_2^{2+}$ | ... | 0.8 |

composition of metastable $CF_4^{+*}$ ions.[19] From this *in situ* observation of the metastable dissociation process $CF_4^{+*} \rightarrow CF_3^+ + F$ a previous suggestion by Brehm *et al.*[5] is confirmed, i.e., not only prompt dissociation of $CF_4^+$ ($X\,^2T_1$) and $CF_4^+$ ($A\,^2T_2$) but also metastable dissociation processes are responsible for the absence of observable $CF_4^+$ in a mass spectrum. Additional information on metastable fragment ions comes from a recent study by Proctor *et al.*[20]

### A. Absolute partial ionization cross section functions

The absolute partial ionization cross sections obtained in the present study are shown in Fig. 8 as a function of electron energy. A representative set of values of the cross sections determined are given in Table II. No cross sections are reported for the production of $CF^{2+}$, because the small signal available is not allowing a meaningful calibration. The maximum relative error is estimated to be $\pm$ 5% for singly charged fragment ions, and $\pm$ 10% for doubly charged fragment ions, whereas for the absolute values an error of $\sim \pm$ 10% has to be assumed.

To the authors' knowledge no previous determination exists of these cross section functions. There is only one study reporting the ratio of ion currents at one particular electron energy[10] using a 180° mass spectrometer operated under conventional conditions. Moreover, Dibeler *et al.*[10] have obtained the kinetic energy distribution of $CF_3^+$ and $CF_2^+$ ions from $CF_4$ (using the beam deflection method of Berry[21]) clearly showing definite breaks and broadening in the kinetic energy distribution due to excess kinetic energy in agreement with the present results shown in Figs. 2 and 3. A comparison between ion current ratios reported by Dibeler *et al.*[10] and our data is given in Table III, in which values of $CF_3^+$ have been set to 100. The large values reported by Dibeler *et al.*[10] for the fragment ions smaller than $CF_3^+$ could be due to the minimum in the $z$ ion beam shape (e.g., see Fig. 3) of the reference ion $CF_3^+$ leading to an underestimation of the $CF_3^+$ ion current if no integration over ion beam profiles is performed.

### B. Absolute total and counting ionization cross sections

The sums of the absolute partial ionization cross sections of all fragment ions gives the absolute counting ionization cross section (Fig. 9), whereas the charge weighted sum of the absolute partial ionization cross sections (summation method[1]) gives the absolute total ionization cross section (see Fig. 8). A representative set of values of both cross sections is given in Table II. The relative error of these cross sections is estimated to be $\sim \pm$ 5%, whereas for the absolute values an error of $\sim \pm$ 10% has been estimated due to uncertainties in the calibration procedure.

Also shown in Fig. 8 are values reported by Beran and Kevan[11] for the total ionization cross section measured at 70, 35, and 20 eV, respectively. Beran and Kevan[11] have measured total ionization cross sections for a number of gases for 70 eV electrons. Their results appear to be systematically larger as compared to the established data[1] of Rapp and Englander-Golden.[17] Beran and Kevan[11] report the same ionization cross section for $CH_4$ and for $CF_4$ at 70 eV. If one assumes that the cross section for $CH_4$ as reported by Rapp and Englander-Golden[17] is correct and if one assumes on the basis of Beran and Kevan's results that the cross section for

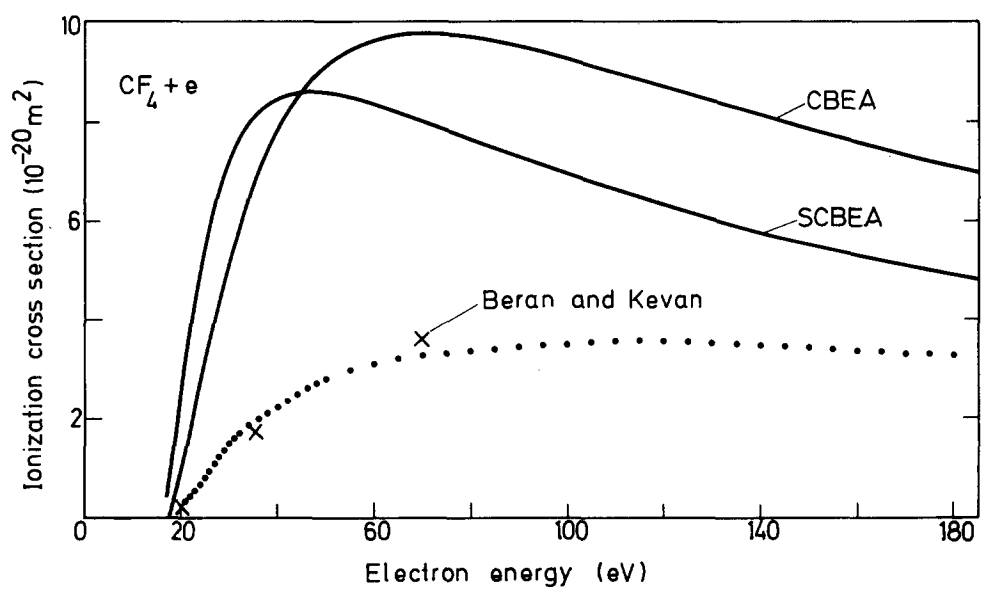


FIG. 9. Absolute (counting) ionization cross section function of $CF_4$. Curve CBEA: calculated values using classical binary encounter approximation after Gryzinski (Ref. 22) [see Eq. (39) in Ref. 1], Curve SCBEA: calculated values using semiclassical binary encounter approximation after Burgess (Ref. 23) and Vriens (Ref. 24) [See Eq. (41) in Ref. 1] and full dots experimental results of the present study. Also shown (crosses) total ionization cross sections reported by Beran and Kevan (Ref. 11) recalibrated with help of data reported by Rapp and Englander-Golden (Ref. 17) (see the text).

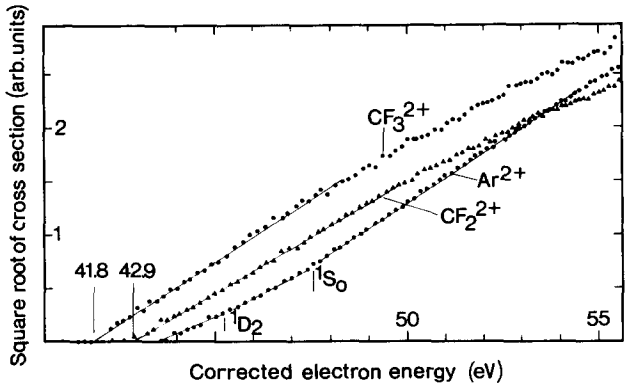


FIG. 10. Square root of the double ionization cross section $q(Ar^{2+}/Ar)$, $q(CF_3^{2+}/CF_4)$ and $q(CF_2^{2+}/CF_4)$ as a function of electron energy near threshold.

$CH_4$ is equal to that of $CF_4$, the total ionization cross section for $CF_4$ at 70 eV would be $\sim 3.6\times10^{-20}$ m$^2$, at 35 eV $\sim 1.7\times10^{-20}$ m$^2$, and at 20 eV $\sim 0.20\times10^{-20}$ m$^2$, respectively. These values are in good agreement with the present determination (see Fig. 8). According to Winters and Inokuti[12] the total cross section for dissociation is $5.1\times10^{-20}$ m$^2$ at 70 eV and therefore ionization events appear in accordance with these authors to account for $\sim 70\%$ of all dissociative events.

In addition, there exist several estimates of the absolute total ionization cross section of $CF_4$. Recently Fitch and Sauter[25] have given a value for $CF_4$ (at 70–75 eV) based on the additivity of atomic total ionization cross sections as proposed by Otvos and Stevenson.[26] Their value (recalibrated to the more accurate data of Rapp and Englander-Golden[17]) of $3.4\times10^{-20}$ is in excellent agreement with the present results of $3.28\times10^{-20}$ m$^2$ at 70 eV and $3.33\times10^{-20}$ at 75 eV.

Moreover, we have calculated absolute counting ionization cross section functions for $CF_4$ using a classical binary encounter approximation method[22] and a semiclassical binary encounter approximation method[23–24] [using the formulas given in Ref. 1 and the ionization energies given by Potts *et al.*[27] for $1t_1 = 16.23$ eV, $4t_2 = 17.47$ eV, $1e = 18.50$ eV, $3t_2 = 21.95$ eV, and $4a_1 = 25.1$ eV, respectively (see also a recent angle-resolved photo electron study by Carlson *et al.*[28])]. Figure 9 gives a comparison of experimental and theoretical values of the counting ionization cross sections. It can be seen that the calculations give values which are much too large, a behavior which has been also observed recently for $CCl_4$[4] (see also a recent review by Deutsch and Schmidt[29] on the quantitative determination of ionization cross sections).

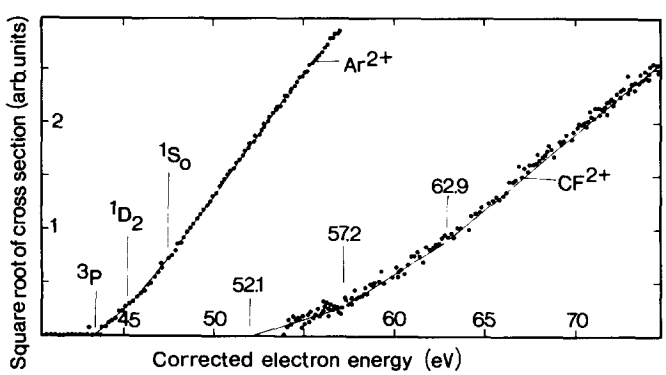


FIG. 11. Square root of the double ionization cross section $q(Ar^{2+}/Ar)$ and $q(CF^{2+}/CF_4)$ as a function of electron energy near threshold.

TABLE IV. Appearance energies in eV for doubly-ionized fragment ions in $CF_4$.

| Ion | Present | Bibby *et al.* (Ref. 9) |
|---|---|---|
| $CF_3^{2+}$ | $41.8 \pm 0.3$ | $42.7 \pm 0.3$ |
| $CF_2^{2+}$ | $42.9 \pm 0.3$ | $44.3 \pm 0.3$ |
| $CF^{2+}$ | $52.1 \pm 0.5$ | ... |

### C. Appearance energies

Appearance energies of singly charged $CF_4$ fragment ions have been measured by several authors previously.[8] To the authors' knowledge only one experimental determination of appearance energies for the doubly charged fragment ions $CF_3^{2+}$ and $CF_2^{2+}$ in $CF_4$ (see also Ref. 30) and none for $CF^{2+}$ is available.[9] On the basis of the $n$th power threshold rule,[1,8] the appearance energy for double ionization is taken in the present study as the point at which the extrapolated square root of the double ionization cross section function meets the electron energy axis (e.g., see Figs. 10 and 11). Argon was used as reference gas with a value for the ionization energy $Ar^{2+} = 43.4$ eV.[8] As reported previously,[31] the square root of the argon cross section curve exhibits—if the energy resolution is good enough—changes in slopes which can be correlated to the onset of the energy states in this region: $3p^4\ ^1D_2$ and $3p^4\ ^1S_0$ (see Figs. 10 and 11).

Moreover, it can be seen that for the doubly charged fragment ions of $CF_4$ a square law dependence of the cross sections has been found from threshold up to some 10 eV above threshold in agreement with results for other doubly charged fragment ions, most notably $CCl_4$.[4] Extrapolating this long square root behavior to the energy axis yields for $CF_3^{2+}$ an appearance energy of $41.8 \pm 0.3$ eV and for $CF_2^{2+}$ of $42.9 \pm 0.3$ eV, respectively (Fig. 10). In the case of $CF^{2+}$ there seem to be changes of slope in the square root function (similar to $Ar^{2+}$), yielding a lowest appearance energy of $52.1 \pm 0.5$ eV and two breaks at 57.2 and 62.9 eV, respectively (see Fig. 11). The present results do not agree with the values shown in Table IV reported in a previous study[9]; it may be assumed however, that similar to $CCl_4$,[4] a linear extrapolation was used to determine these earlier values, which would explain the higher thresholds observed by Bibby *et al.*[9]

## ACKNOWLEDGMENT

Work partially supported by the Österreichischer Fonds zur Förderung der Wissenschaftlichen Forschung.

[1]T. D. Märk, in *Electron Molecule Interactions and Their Applications*, edited by L. G. Christophorou (Academic, Orlando, 1984) Vol. 1, Chap. 3, pp. 251–334; T. D. Märk and G. H. Dunn, *Electron Impact Ionization* (Springer, Wien, 1985).
[2]D. L. Flamm and V. L. Donnelly, Plasma Chem. Plasma Proc. **1**, 317 (1981), and references therein.
[3]H. U. Poll and H. Schlemm, Beitr. Plasmaphys. **22**, 195 (1982); R. d'Agostino, F. Cramarossa, and S. De Benedictis, Plasma Chem. Plasma Proc., **2**, 213 (1982); W. W. Brandt and P. Roselle, *ibid.* **3**, 337 (1983).
[4]K. Leiter, K. Stephan, E. Märk, and T. D. Märk, Plasma Chem. Plasma Proc. **4**, 235 (1984).
[5]B. Brehm, R. Frey, A. Küstler, and J. H. D. Eland, Int. J. Mass. Spectrom. Ion Phys. **13**, 251 (1974), and references therein.
[6]J. E. Ahnell and W. S. Koski, J. Chem. Phys. **62**, 4474 (1975), and references therein.
[7]See e.g., H. A. Van Sprang, H. H. Brogersma, and F. J. de Heer, Chem. Phys. **35**, 51 (1978); J. P. Maier and F. Thommen, Chem. Phys. Lett. **78**, 54 (1981); R. Cambi, G. Ciullo, A. Sgamellotti, F. Tarantelli, R. Fantoni, A. Giardini-Guidoni, M. Rosi, and R. Tiribelli, *ibid.* **90**, 445 (1982).
[8]H. M. Rosenstock, K. Draxl, B. W. Steiner, and J. T. Herron, J. Phys. Chem. Ref. Data **6**, Suppl. 1 (1977).
[9]M. M. Bibby, B. J. Toubelis, and G. Carter, Electron. Lett. **1**, 50 (1965).
[10]V. H. Dibeler, R. M. Reese, and F. L. Mohler, J. Res. Natl. Bur. Stand. **57**, 113 (1956).
[11]J. A. Beran and L. Kevan, J. Phys. Chem. **73**, 3866 (1969).
[12]H. F. Winters and M. Inokuti, Phys. Rev. A **25**, 1420 (1982).
[13]R. C. Wetzel, F. A. Baiocchi, and R. S. Freund, 37th GEC, Boulder Co. (1984).
[14]K. Stephan, H. Helm, and T. D. Märk, J. Chem. Phys. **73**, 3763 (1980).
[15]L. J. Kieffer and G. H. Dunn, Rev. Mod. Phys. **38**, 1 (1966).
[16]C. Brunnee and H. Voshage, *Massenspektrometrie* (Thiemig, München, 1964).
[17]D. Rapp and P. Englander-Golden, J. Chem. Phys. **43**, 1464 (1965).
[18]T. D. Märk, J. Chem. Phys. **63**, 3731 (1975).
[19]H. Deutsch, K. Leiter, and T. D. Märk, Int. J. Mass Spectrom. Ion Proc. (in press).
[20]C. J. Proctor, C. J. Porter, T. Ast, and J. H. Beynon, Int. J. Mass Spectrom. Ion Phys. **41**, 251 (1982).
[21]C. E. Berry, Phys. Rev. **78**, 597 (1950).
[22]M. Gryzinski, Phys. Rev. A **138**, 305, 322, 336 (1965).
[23]A. Burgess, Proc. 3rd ICPEAC, London (1963), p. 237.
[24]L. Vriens, Phys. Rev. **141**, 88 (1966).
[25]W. L. Fitch and A. D. Sauter, Anal. Chem, **55**, 832 (1983).
[26]J. W. Otvos and D. P. Stevenson, J. Am. Chem. Soc. **78**, 546 (1956).
[27]A. W. Potts, H. J. Lempka, D. G. Streets, and W. C. Price, Philos, Trans. R. Soc. London Sect. A **268**, 59 (1970).
[28]T. A. Carlson, A. Fahlman, W. A. Svensson, M. O. Krause, T. A. Whitley, F. A. Grimm, M. N. Piancastelli, and J. W. Taylor, J. Chem. Phys. **81**, 3828 (1984).
[29]H. Deutsch and M. Schmidt, Beitr. Plasmaphys. **24**, 475 (1984).
[30]D. M. Curtis and J. H. D. Eland, Int. J. Mass. Spectrom. Ion Proc. **63**, 241 (1985).
[31]K. Stephan, H. Helm, Y. B. Kim, G. Sejkora, J. Ramler, M. Grössl, E. Märk, and T. D. Märk, J. Chem. Phys. **73**, 303 (1980); and T. D. Märk, E. Märk, and K. Stephan, *ibid.* **74**, 1728 (1981).